

Article

Spontaneous Release of Metalloradicals and Coordinatively Unsaturated Species in Asymmetric Iridium Dimers to Promote C-N Bond Formation

Tsun-Ren Chen *, Yi-Sheng Chen, Chia-Ying Li , Yen-Hsing Lin and Yu-Tung Chen

Department of Applied Chemistry, National Pingtung University, Pingtung 90003, Taiwan

* Correspondence: trchen@mail.nptu.edu.tw; Tel.: +886-9-33261376

Abstract: An unusual iridium dimer **1**, [(4-cpbo)Ir(μ -Cl)(μ -O)Ir(4-cpbo)] (4-cpbo = 4-chlorophenylbenzoxazolato-N,C²), was obtained by the oxidative addition of oxygen and reductive elimination of chlorine from a precursor [(4-cpbo)₂Ir(μ -Cl)]₂. This iridium dimer **1** has a metastable structure with an asymmetric bridge, can spontaneously release metalloradicals and coordinatively unsaturated species in solution at room temperature, and exhibits high catalytic ability for synthetic applications.

Keywords: iridium; C-N bond formation; metalloradical; coordinatively unsaturated; catalysis



Citation: Chen, T.-R.; Chen, Y.-S.; Li, C.-Y.; Lin, Y.-H.; Chen, Y.-T. Spontaneous Release of Metalloradicals and Coordinatively Unsaturated Species in Asymmetric Iridium Dimers to Promote C-N Bond Formation. *Inorganics* **2022**, *10*, 237. <https://doi.org/10.3390/inorganics10120237>

Academic Editors: Franz Edwin López Suárez, Robison Buitrago and Andres F. Suárez

Received: 5 November 2022

Accepted: 1 December 2022

Published: 2 December 2022

Publisher's Note: MDPI stays neutral with regard to jurisdictional claims in published maps and institutional affiliations.



Copyright: © 2022 by the authors. Licensee MDPI, Basel, Switzerland. This article is an open access article distributed under the terms and conditions of the Creative Commons Attribution (CC BY) license (<https://creativecommons.org/licenses/by/4.0/>).

1. Introduction

It is well known that metal radicals and coordinatively unsaturated species play important roles in various fields, including energy transfer in biological systems, pharmaceutical research, and synthetic chemistry [1–3]. Various topics have been discussed in order to study the application of metal radicals and coordinatively unsaturated species, most of which focused on the study of group 9 metal complexes [4–9]. Although rare, other elements have also been explored, such as nickel [10,11], iron [12], and copper complexes [13,14]. One of the most important properties of metalloradical is metalloradical catalysis (MRC), which leads to a diversity of catalytic reactions, such as C–H activation, H–H activation, and C–H amination [15–17]. Complexes with vacant coordination are also widely used to catalyze oxidative addition and reductive elimination reactions. In most cases, metal radicals and coordinatively unsaturated species are generated by the dissociation of some unstable molecules, for example, by chemical, photochemical, or electrochemical reactions [18,19]. The formation of these reactive species at ambient temperature without additional reaction conditions is rarely observed, but it is important. In 1988, the concept of 18+ δ was reported, where the value of δ represents the fraction of electrons that are located in the metal center [20]. Because 18+ δ complexes often undergo further reactions, such as ligand dissociation, reduction, or oxidation of metal atoms, etc., the synthesis and separation of such complexes are relatively difficult, and there are few reports on 18+ δ complexes [21–23]. In this report, we discovered a novel diiridium compound with an 18+ δ structure, a metastable structure with an asymmetric bridge, which can spontaneously release metalloradicals and coordinatively unsaturated species in solution at room temperature and exhibits high catalytic ability for C-N bond formation.

Organic nitrogen compounds are essential components and play a vital role in bioactive compounds. The construction of nitrogen-containing organic groups is an important technology in the fields of organic synthetic chemistry, medicine, and fine chemical industry. The C-N bond formation is traditionally carried out by the alkylation of amines with alkyl halides, which is usually fast but has significant disadvantages [24,25]. For example, excessive alkylation leads to lower yields of desired product, and side reactions lead to complicated purification procedures. To date, there are many improved methods for C-N bond formation, including hydroamination [26,27], Ullmann reactions [28,29], and Buchwald–Hartwig coupling [30,31]. Recently, several reports have demonstrated a

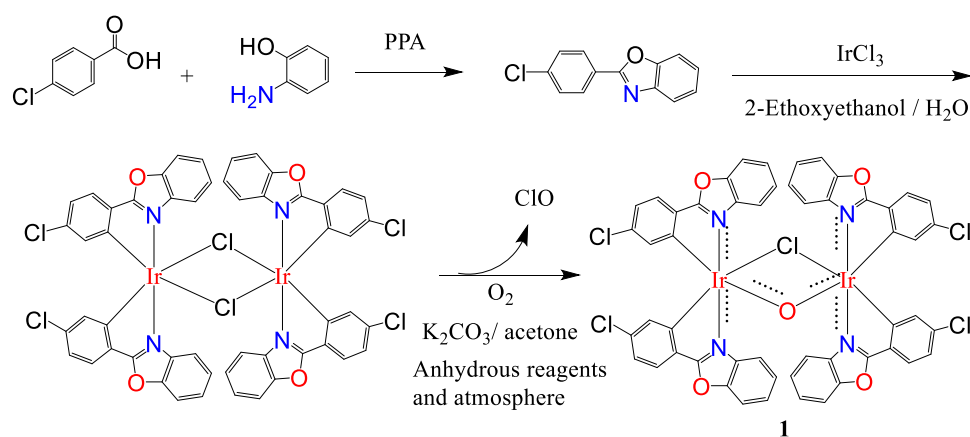
robust and sustainable approach to forming new C–N bonds using a catalytic hydrogen autotransfer (HA) strategy by using less toxic and more readily available alcohols as alkylating agents [32–34]. Additionally, various amine N-alkylation catalysts using alcohols as alkylating agents have been discovered, the most common of which are iridium [35–37] and ruthenium [38,39] complexes, and many others have been explored [40,41]. Most of these studies report useful catalytic systems, but most of them must use bases, solvents, and other additives, which limits the development of these truly green process proposals.

In this report, we introduce an asymmetric iridium dimer as a catalyst for the N-alkylation of amines to prepare nitrogen-containing derivatives and heterocyclic compounds. The catalyst can directly promote the formation of C–N bonds without preactivation steps and additives such as solvents and bases. In the reaction system, the only by-product is water, which can be used in tandem reactions or specific intermolecular cyclization reactions to construct biologically active drugs or other specific applications.

2. Results and Discussion

2.1. Synthesis and Structural Characterization

Reaction of $[(4\text{-cpbo})_2\text{Ir}(\mu\text{-Cl})_2]$ (4-cpbo = 4-chlorophenylbenzoxazolato- N,C^2) with oxygen in anhydrous acetone and a catalytic amount of anhydrous potassium carbonate produces the unusual iridium dimer $[(4\text{-cpbo})\text{Ir}(\mu\text{-Cl})(\mu\text{-O})\text{Ir}(4\text{-cpbo})]$ (**1**) (Scheme 1).



Scheme 1. Synthetic route to ligand 4-cpbo, iridium dimers $[(4\text{-cpbo})_2\text{Ir}(\mu\text{-Cl})_2]$, and complexes **1**.

A single-crystal X-ray structure determination confirmed the dimeric nature of **1** (Figure 1). The diffraction data of complex **1** was collected on a Bruker SMART APEX CCD diffractometer with graphite-monochromatized Mo $K\alpha$ X-ray radiation ($\lambda = 0.71073 \text{ \AA}$) at 150K. All calculations for the structure determination were carried out using SHELXTL package (version 5.1). The positions of the heavy atoms, including the iridium atoms, were located by the direct method. The remaining atoms were found in a series of alternating difference Fourier maps and least-square refinement [6]. Crystal data for compound **1**: formula $\text{C}_{52}\text{H}_{28}\text{Cl}_5\text{Ir}_2\text{N}_4\text{O}_5 \cdot 2((\text{CH}_3)_2\text{CO})$, $M = 1466.59$, Monoclinic, space group $P 21/c$, $a = 12.7868 (5)$, $b = 21.2778 (8)$, $c = 21.4635 (8) \text{ \AA}$, $V = 5676.5(4) \text{ \AA}^3$, $Z = 4$, $\rho_{\text{calc}} = 1.716 \text{ gcm}^{-3}$, $F(000) = 2844$, $T = 150(2) \text{ K}$, $2\theta_{\text{max}} = 29.392^\circ$, 13,327 reflections collected, 8882 unique, $\text{GooF} = 1.052$, $R_1 = 0.0635$, $wR_2 = 0.1376$. The Ir1–Cl–Ir2, Ir1–O–Ir2, Cl–Ir1–O, and Cl–Ir2–O angles are $87.76 (11)$, $105.0 (3)$, $83.49 (17)$, and $83.62 (17)^\circ$, respectively. The dihedral angle between Ir1–Cl–Ir2 and Ir1–O–Ir2 is 4.9° . Crystallographic information indicates that complex **1** has an asymmetric bridge connecting the two iridium nuclei, and the selected bond distances and bond angles are listed in Table 1.

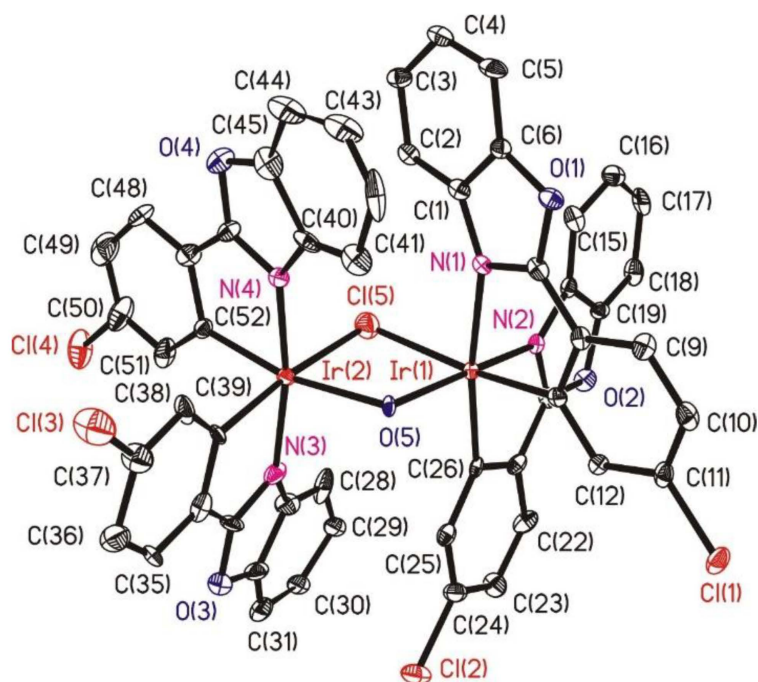


Figure 1. ORTEP plots of **1**. Thermal ellipsoids are drawn at the 30% probability level and hydrogen atoms are omitted for clarity.

Table 1. Selected Bond Distance (Å) and Bond Angles for Compound **1**.

Bond Distance (Å)			
Ir(1)-N(1)	2.157 (7)	Ir(1)-N(2)	2.049 (7)
Ir(1)-C(13)	2.011 (9)	Ir(1)-C(26)	2.035 (9)
Ir(1)-Cl(5)	2.457 (3)	Ir(1)-O(5)	2.093 (5)
Ir(2)-N(3)	2.069 (8)	Ir(2)-N(4)	2.037 (7)
Ir(2)-C(39)	2.021 (9)	Ir(2)-C(52)	2.022 (10)
Ir(2)-Cl(5)	2.402 (3)	Ir(2)-O(5)	2.153 (5)
Bond Angles (°)			
Ir(1)-Cl(5)-Ir(2)	87.76 (11)	Ir(1)-O(5)-Ir(2)	105.0 (3)
C(13)-Ir(1)-C(26)	92.7 (3)	C(39)-Ir(2)-C(52)	94.7 (4)
N(1)-Ir(1)-N(2)	95.8 (3)	N(3)-Ir(2)-N(4)	170.5 (3)
C(26)-Ir(1)-N(1)	171.9 (3)	C(39)-Ir(2)-N(3)	79.5 (4)
C(13)-Ir(1)-Cl(5)	170.4 (3)	C(39)-Ir(2)-Cl(5)	173.5 (3)
O(5)-Ir(1)-Cl(5)	83.49 (17)	O(5)-Ir(2)-Cl(5)	83.62 (17)
N(2)-Ir(1)-O(5)	171.6 (2)	C(52)-Ir(2)-O(5)	167.7 (3)

Electron paramagnetic resonance (EPR) spectra of iridium complex **1** crystals were recorded at 77 and 298 K and in dichloromethane solution at 298 K (Figure 2). The low temperature EPR spectrum of complex **1** crystal displays rhombic symmetry with $g_x = 2.017$, $g_y = 1.994$, and $g_z = 1.922$ (Figure 2a). The unresolved hyperfine structure is significantly broadened, indicating that the unpaired electron is localized on a mixed orbital composed of ligand pi and metal d orbitals. At room temperature, the crystal of complex **1** shows an EPR pattern similar to that at 77K, but the g-tensor component moves significantly ($g_x = 1.927$, $g_y = 1.907$, and $g_z = 1.845$, Figure 2b), indicating that the distribution of the unpaired electrons remains unchanged, but as the temperature increases, the microenvironment of the complex **1** crystal is affected. The solution of complex **1** at 298 K shows more complicated EPR signals (Figure 2c). The g factors are 2.228, 1.934, 1.917, 1.912, and 1.901, respectively, indicating that new free radicals are released in the solution.

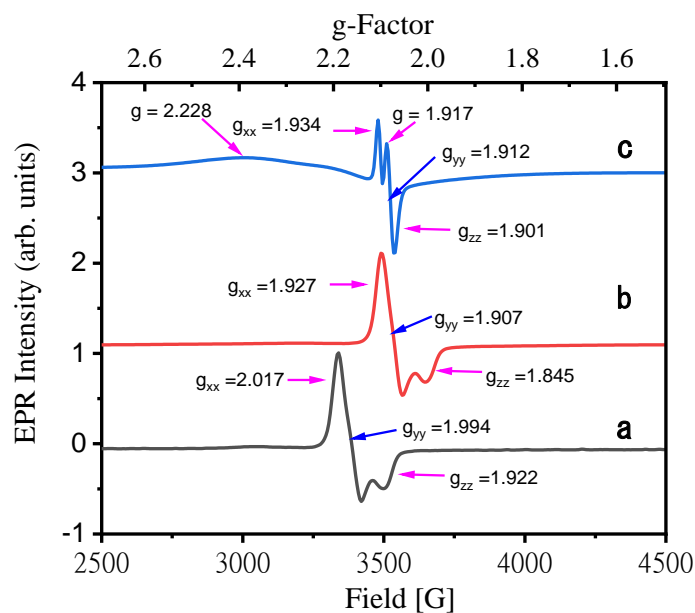


Figure 2. EPR spectra of **1**: (a) crystal at 77K, (b) crystal at 298K, and (c) solution in dichloromethane at 298 K. EPR settings: microwave frequency, 9.879 GHz; microwave power, 10.080 mW; number of scans, 1.

Theoretical calculations used Becke's three-parameter B3LYP for C, H, O, N, and Cl, and the LANL2DZ basis set for the element Ir used the package Gaussian 03. The atomic coordinates of the complexes were obtained directly from X-ray crystallography and used as the initial geometry for optimization. The metric parameters obtained from the X-ray structure and DFT calculations are in good agreement (Table 2), and the atomic coordinates (Angstroms) of complex **1** are listed in Supplementary Materials Table S1. The calculated single-molecular orbital (SOMO) of compound **1** is composed of 87.91% $\pi(4cpbo)$ + 10.53% $d(Ir)$ + 1.34% ($\mu-O$) + 0.3916% ($\mu-Cl$) (Figure 3). This is consistent with the EPR spectrum observation of the crystal of complex **1**, where the unpaired electrons are delocalized to iridium, $\mu-O$, $\mu-Cl$, and two ligands 4cpbo. This delocalization stabilizes the structure of **1** and leads to the isolation of this compound.

Table 2. Comparison of selected bond lengths (Å) and angles (°) of **1** from crystallography and DFT calculation.

	Ir-Cl	Ir-O	Ir-N	Ir-C
X-ray	2.457 (3)	2.153 (5)	2.157 (7)	2.035 (9)
	2.402 (3)	2.093 (5)	2.069 (8)	2.022 (10)
			2.049 (7)	2.021 (9)
			2.037 (7)	2.011 (9)
DFT	2.454	2.150	2.154	2.031
	2.309	2.090	2.065	2.017
			2.045	2.016
			2.033	2.008

To double check, XPS tests were performed to explore the oxidation states of iridium ions. The Ir 4f XPS spectrum of complex **1** shows Ir $4f_{7/2}$ (59.88 eV) and Ir $4f_{5/2}$ (62.89 eV) peaks (Figure 4a). Compared with the spectrum of $[(4cpbo)_2Ir^{III}(\mu-Cl)]_2$ (Figure 4b) (Ir $4f_{7/2}$ = 59.53 eV, Ir $4f_{5/2}$ = 62.54 eV), the XPS spectrum of complex **1** shifted by about 0.35 and 0.46 eV toward higher binding energies. Compared with the spectrum of $[(dcpbo)_2Ir^{IV}(\mu-O)]_2$ (Figure 4c) (Ir $4f_{7/2}$ = 60.04 eV, Ir $4f_{5/2}$ = 63.08 eV), the XPS spectrum of complex **1** shifted by about 0.05 and 0.19 eV toward slightly lower binding energies. The comparison of XPS spectra of iridium complexes shows that the oxidation state of iridium ion in **1** is higher than +3 but close to +4.

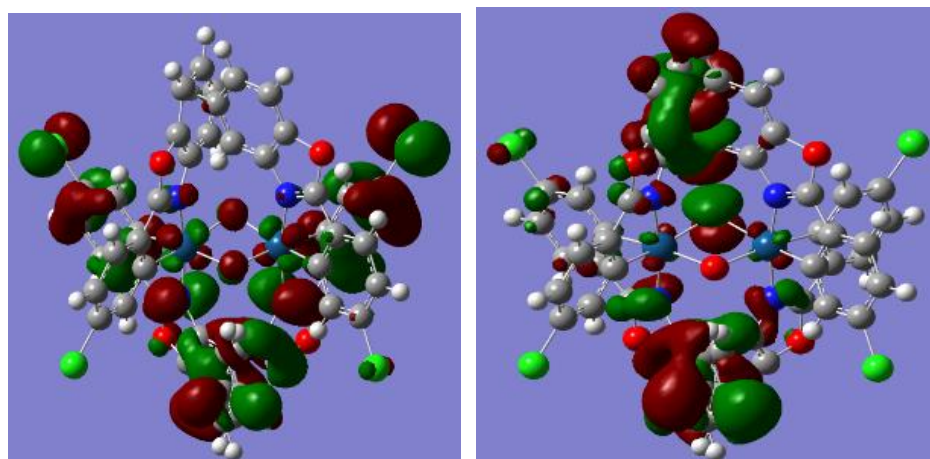


Figure 3. Electron density of the SOMO (left) and LUMO (right) in $[(4cpbo)_2Ir]_2(\mu-Cl)$.

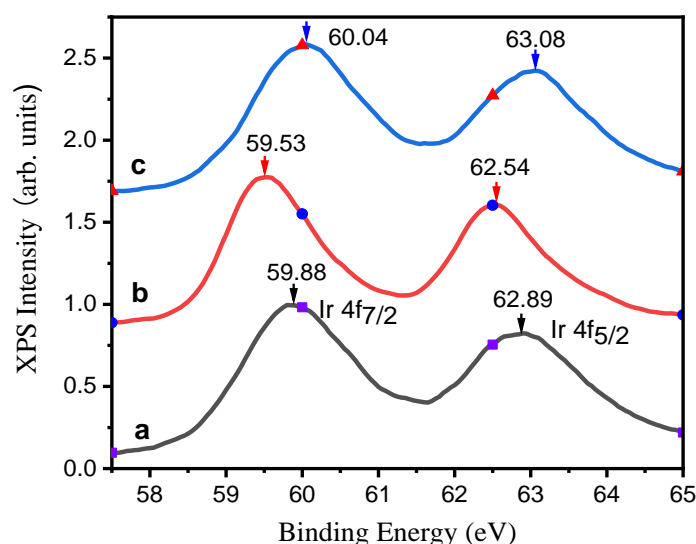


Figure 4. Ir 4f XPS spectra of (a) compound **1**, (b) $(4cpbo)_2Ir^{III}(\mu-Cl)$, and (c) $[(dfpbo)_2Ir^{IV}(\mu-O)]_2$.

The (FAB+) (Fast Atom Bombardment) spectrum of **1** (Figure 5) shows medium-intensity complex patterns of $[(4cpbo)_2IrO] \bullet^+$ [$^{191}Ir, ^{35}Cl$ m/z 663 (6.36%), $^{193}Ir, ^{35}Cl$ m/z 665 (10.47%), $^{191}Ir, ^{37}Cl$ m/z 667 (7.35%), and $^{193}Ir, ^{37}Cl$ m/z 669 (2.52%)] and $[(4cpbo)_2IrO+H] \bullet^+$ [$^{191}Ir, ^{35}Cl$ m/z 664 (7.24%), $^{193}Ir, ^{35}Cl$ m/z 666 (10.79%), $^{191}Ir, ^{37}Cl$ m/z 668 (5.56%), and $^{193}Ir, ^{37}Cl$ m/z 670 (1.40%)]. The low-intensity complex patterns of $[(4cpbo)_2IrCl] \bullet^+$ [$^{191}Ir, ^{35}Cl, ^{35}Cl$ m/z 682 (1.4%), $^{193}Ir, ^{35}Cl, ^{35}Cl$ m/z 684 (1.65%), $^{191}Ir, ^{35}Cl, ^{37}Cl$ m/z 686 (1.39%)] and $[(4cpbo)_2IrCl+H] \bullet^+$ [$^{191}Ir, ^{35}Cl, ^{37}Cl$ m/z 687 (1.36%), $^{191}Ir, ^{37}Cl, ^{37}Cl$ m/z 689 (2.06%), and $^{193}Ir, ^{37}Cl, ^{37}Cl$ m/z 691 (2.47%)] were also observed. Which indicates that complex **1** is readily dissociated to form metalloradicals $[(4cpbo)_2IrO] \bullet^+$ and $[(4cpbo)_2IrCl] \bullet^+$. The molecular peak of $[(4cpbo)Ir(\mu-Cl)(\mu-O)Ir(4cpbo)]$ is relatively weak, indicating that complex **1** is easily dissociated. $[(4cpbo)_2Ir(\mu-Cl)]_2$ peak is observed at m/z 1372, which reveal that two metalloradicals $[(4cpbo)_2IrCl] \bullet$ can combine with each other to form a binuclear species, which also explains why the intensity of $[(4cpbo)_2IrCl] \bullet^+$ is much lower than that of $[(4cpbo)_2IrO] \bullet^+$.

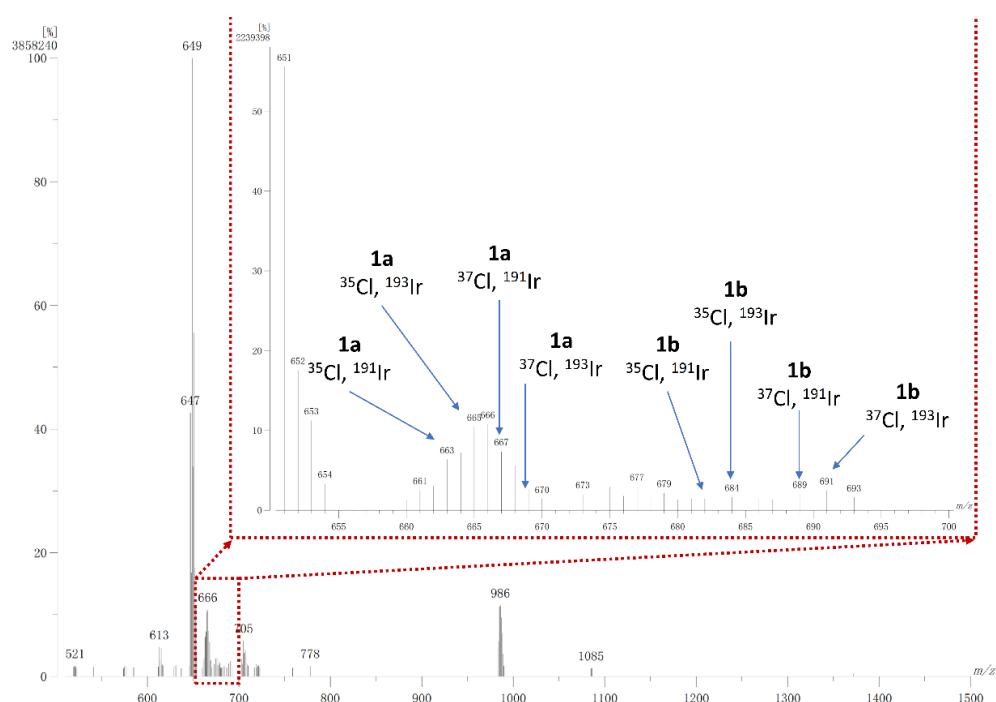
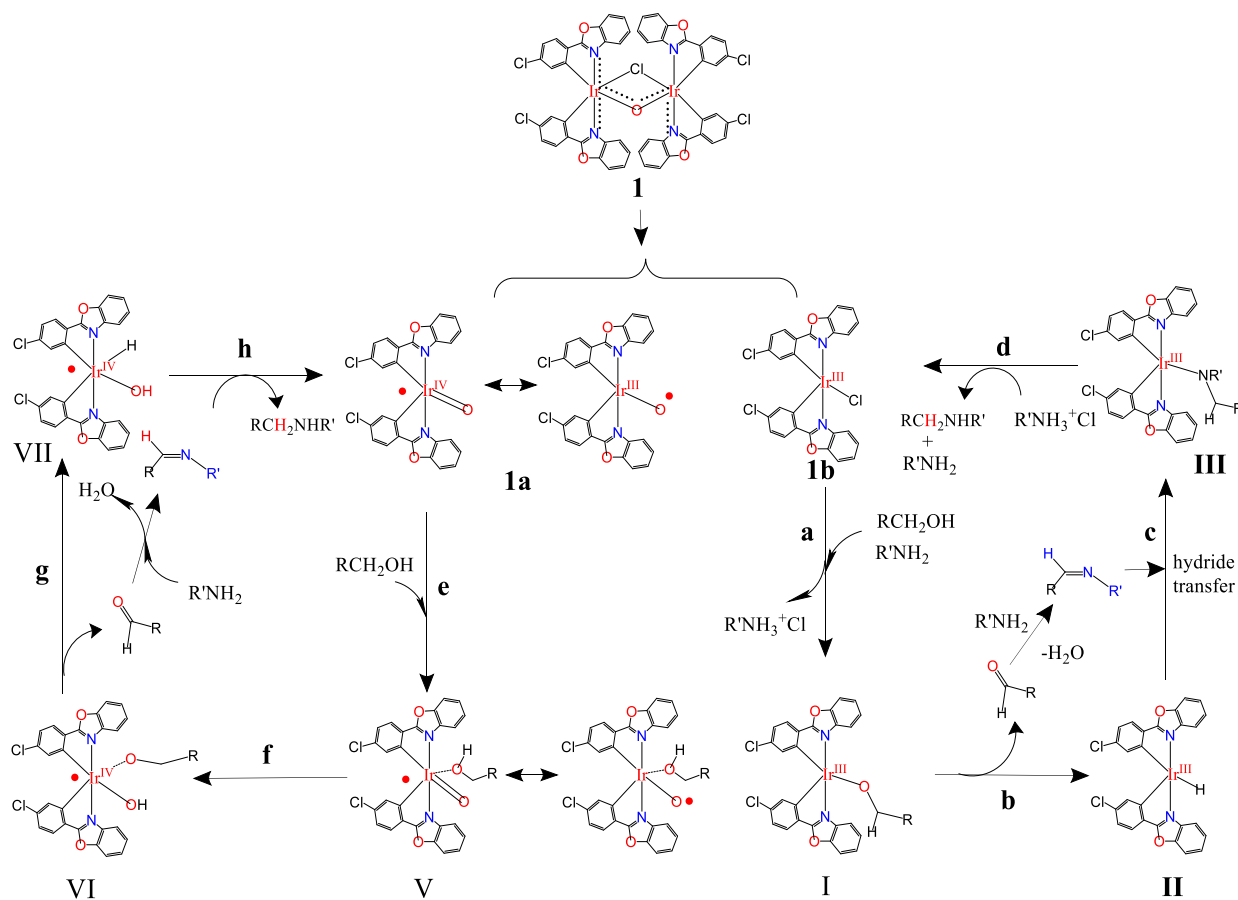


Figure 5. Mass spectrum of **1** with fast atom bombardment.

The above information indicates that the asymmetric bridged dimer complex **1** has an unpaired electron delocalized throughout the molecule, which can dissociate in solution to release various mononuclear iridium species, including an iridium radical (**1a**) and a mononuclear iridium complex with a vacant coordination site (**1b**) (Scheme 2). Both metallic radicals and coordinatively unsaturated species can activate a variety of chemical bonds, such as carbon–hydrogen bond activation (CHA) and carbon–carbon bond activation (CCA), which has been widely studied and used in various applications such as metathesis, polymerization, C–C bond formation, and C–N bond formation. Here, complex **1** is catalytically active for C–N bond formation. The alcohol binds to the vacant coordination site of **1b** and is then deprotonated by the extra amine, resulting in the dissociation of ammonium chloride to give the coordinatively unsaturated Ir-alkoxide complex I (step a). Then, β -hydride elimination occurs to give an Ir(III)-hydride complex II and an aldehyde (step b). Dehydration condensation of aldehydes and amines yields imine intermediate, which is attacked by Ir-hydrides to yield Ir-amide intermediates III (step c). Finally, protonation by ammonium chloride furnishes the catalytic cycle to generate alkylated amines and a recovered Ir catalyst (step d). For the left cycle, the iridium radical (**1a**) traps alcohol in the first step (step e). Then, there is a proton transfer from bound alcohol to oxido ligand, resulting in iridium complex VI with hydroxido and alkoxido ligands (step f). Then, β -hydride elimination occurs to give an iridium complex VII with hydrido and hydroxido ligands and released aldehyde undergoes dehydrative condensation with amine to give imine intermediate (step g). Finally, proton and hydride transfer from iridium-hydride and -hydroxide complex to imine yields N-alkylation product and recovered iridium complex **1a** (step h).



Scheme 2. Spontaneous release of iridium metalloradical from **1**, and the catalysis of C-N bond formation.

2.2. Initial Catalytic Studies

We carried out a series of catalytic reactions according to different catalyst loading ratios to optimize the catalytic conditions of complex **1**. The ratio of catalyst to amine is in the range of 0.0040 to 0.030 (mmol/mmol) (Cat./aniline), and reactions were placed in Schlenk tubes at 120 °C for 24 h. The composition of the reaction mixture was determined by GC-MS summarized in Figure 6. At a high catalyst loading ratio (0.022 mmol/mmol), the target alkylation product (*N*-benzylaniline) was the main product (>95%), and the over-alkylated product (*N,N*-dibenzylaniline) was the minor product (~4%), and traces of imines (<1%) were observed. At an even higher catalyst loading ratio (0.03 mmol/mmol), the imine disappeared, but the concentration of the target alkylated product decreased (<90%), and the concentration of the over-alkylated product increased significantly (>10%). In contrast, at low loading ratio (0.004 mmol/mmol), the conversion of aniline was very low (~60%), a large amount of intermediates (imines) were observed (~15%), and the concentration of target alkylation product was also low (~45%); therefore, the ideal catalyst loading ratio should be 0.015~0.022 mmol/mmol.

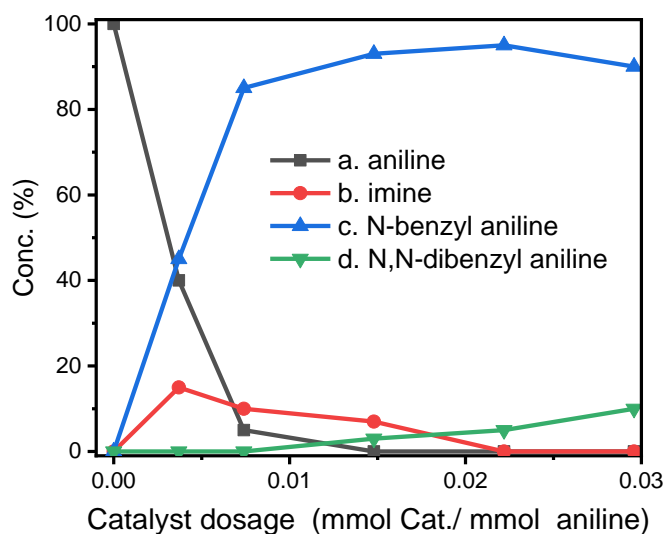


Figure 6. Composition distribution of N-alkylation reaction of aniline and benzyl alcohol under different ratios of catalyst and aniline.

Furthermore, the progression of the N-alkylation reaction showed that the percentage of N-alkylated products increased sharply in the early stage, and intermediate imines were also found (Figure 7). After 24 h of reaction, the concentration of the target product still increased steadily, but the proportion of imine disappeared obviously, indicating that the intermediate imine was rapidly converted into N-alkylated products. After 48 h of reaction, the target alkylated product reached the maximum concentration (95%), and then the over-alkylated product gradually appeared.

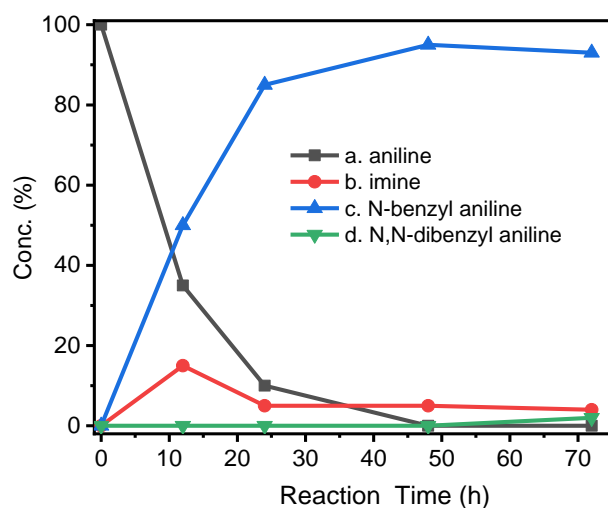
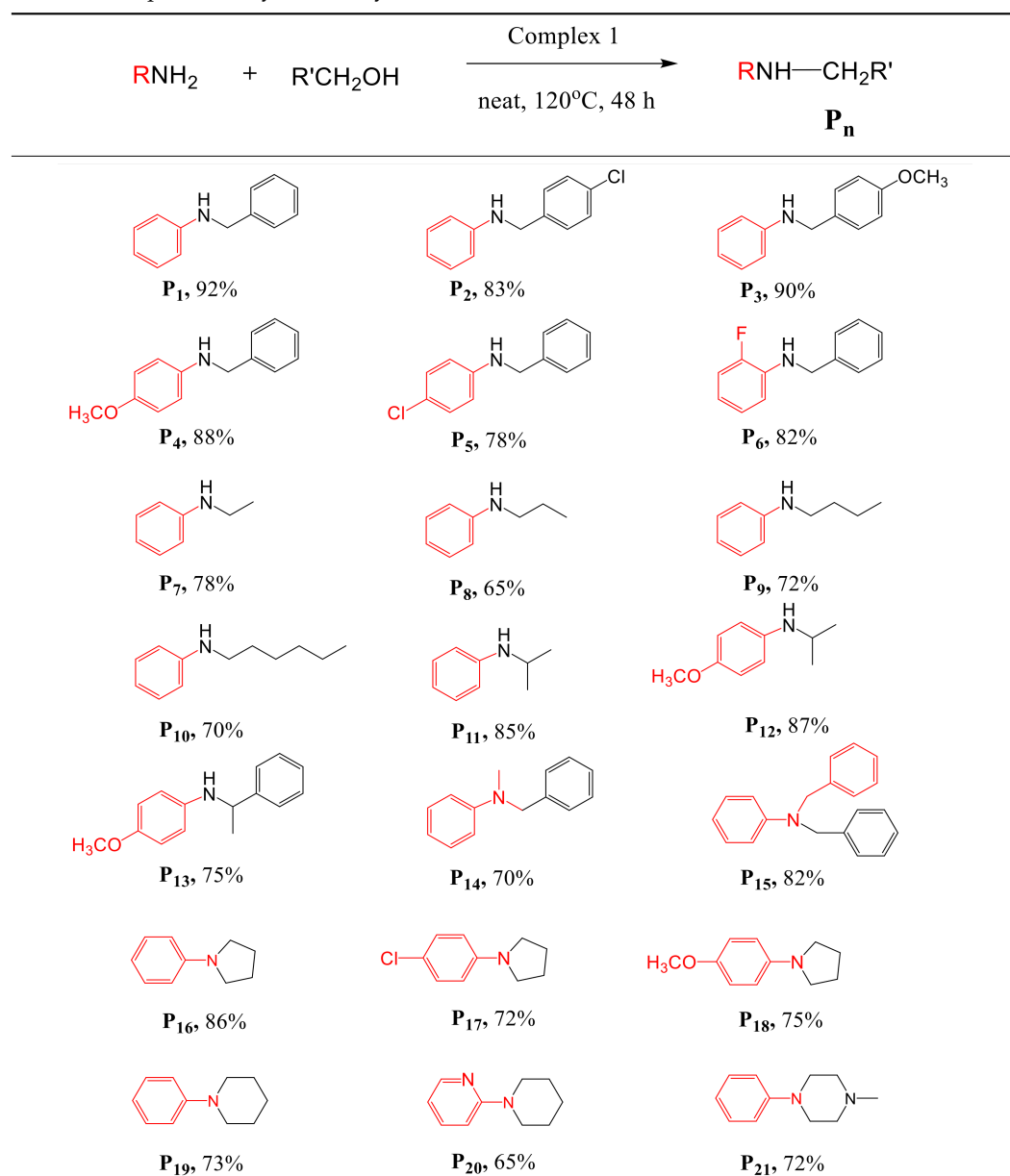


Figure 7. Reaction progress of N-alkylation of aniline. Aniline (1 mmol) reacts with benzyl alcohol (2 mmol) and catalyst (0.018 mmol). Composition distribution of nitrogen-containing products was determined by GC-MS.

2.3. Substrate Scope

Based on the optimized conditions, complex **1** was used to investigate the substrate scope for N-alkylation of amines with alcohols as alkylating reagents (Table 3). First, aniline was alkylated with benzyl alcohol, 4-chlorobenzyl alcohol, and p-anisyl alcohol as alkylating agents. The isolated yields of the secondary amine products P1, P2, and P3 were 92%, 83%, and 90%, respectively.

Table 3. Complex 1 catalyzed N-alkylation of amines.

Amines (1 mmol), alcohols (2 mmol), catalyst (0.018 mmol), without base and solvent, and reaction was carried out at 120 °C for 48 h.

Substituted anilines such as p-anisidine, 4-chloroaniline, and 2-fluoroaniline were also well alkylated by benzyl alcohol to give the corresponding amines P₄, P₅, and P₆ in high yields of 88%, 78%, and 82%, respectively. Although the yields of substrates with electron-withdrawing groups were slightly lower than those with electron-donating groups, they were all within an acceptable range.

We also screened various substrates to assess whether our catalysts could expand the range of N-alkylation of amines with aliphatic alcohols. Thankfully, aliphatic alcohols were successful in alkylating amines with good selectivity and yield, for example, N-alkylation of aniline using ethanol, propanol, butanol, and hexanol as alkylating agents. The yields of products P₇, P₈, P₉, and P₁₀ reached 78%, 65%, 72%, and 70%, respectively.

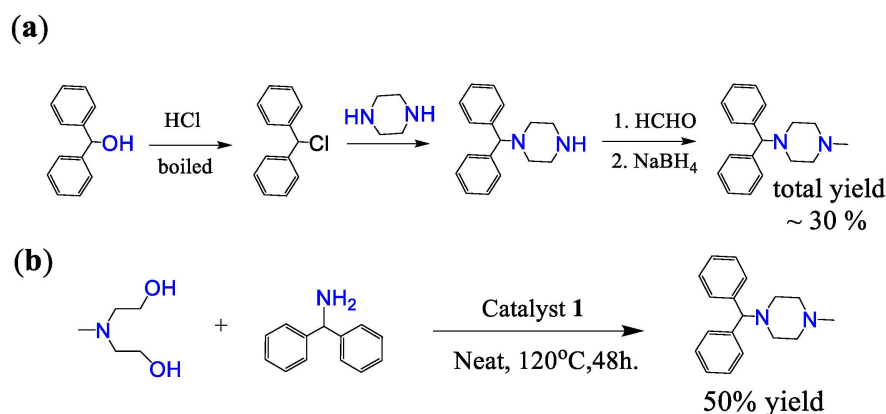
Since the formation of a C-N bond between nitrogen and a secondary carbon is an important step in the construction of some natural products or pharmaceuticals, we constructed this bond by alkylating amines with secondary aliphatic alcohols as alkylating

agents. Interestingly, both aliphatic and aromatic amines can be coupled with secondary aliphatic alcohols. Most of these reactions showed high conversions and good to excellent yields. For example, alkylation of aniline with alcohol (isopropyl alcohol) at 90% conversion yields the corresponding product P₁₁ at 75% yield. Alkylation of 4-methoxyaniline with isopropanol and 1-phenethyl alcohol as alkylating reagents also gave good yields of P₁₂ and P₁₃, 87% and 75%, respectively. Secondary amines were also successfully alkylated; for example, *N*-methylaniline and *N*-benzylaniline were successfully alkylated by benzyl alcohol to give the corresponding products P₁₄ and P₁₅ at 70% and 82% yields, respectively.

In addition, intermolecular cyclization was also achieved through the cyclization reaction of amines with diols. Aniline, 4-chloroaniline, and 4-methoxyaniline were reacted with 1,4-butanediol to form five-membered cyclic amines P₁₆, P₁₇, and P₁₈ at 86%, 72%, and 75% yields, respectively. The reaction of 1,5-pentanediol with different amines gave six-membered cyclized products in good yields, with yields of 70% and 82% for P₁₉ and P₂₀, respectively. Interestingly, by using *N*-substituted diethanolamine, the piperazine derivative (P₂₁) was obtained, which is a phenylpiperazine derivative characterized in that the phenyl group is attached to the piperazine ring. Many phenylpiperazine derivatives are drugs, such as bifepronol, dropromazine, eloprazole, antrafenin, and ciprofloxacin.

2.4. Synthetic Application

Cyclizine is an important drug for the treatment of nausea and dizziness caused by motion sickness or dizziness and is included in the World Health Organization List of Essential Medicines [32,42]. Scheme 3a shows the previously reported preparation of cyclizine, which requires at least four steps and an overall yield of about 30% [43,44]. Many harmful and expensive chemicals must be used, and toxic and ecologically unfavorable substances are released into the environment. In our report, cyclizine was prepared by one-step catalysis using an intermolecular cyclization reaction (Scheme 3b). In a Schlenk tube, *N*-methyldiethanolamine (MDEA) was mixed with diphenylmethanamine and complex 1 and then reacted at 140 °C for 48 h under nitrogen. The product cyclizine was purified by column chromatography, and the isolated yield was 50%, which was good compared with known methods.



Scheme 3. Synthetic route of cyclizine: (a) previous report; (b) our report.

2.5. Conclusions

In summary, we present an unusual iridium compound with an asymmetric bridge that delocalizes unpaired electrons across the molecule and that can dissociate in solution to release various catalytically active species. The compound exhibits diverse catalytic capabilities and good catalytic performance for various reactions, which indicates that it will become an important substance in the exploration of iridium chemistry, catalytic chemistry, and material science.

3. Experimental Section

3.1. Materials and Methods

4-chlorobenzoic acid was purchased from Matrix, and $\text{IrCl}_3 \cdot n\text{H}_2\text{O}$ was from Seedchem Co. All other chemicals were purchased from Acros and used as received. NMR spectra were measured on a Bruker Advance-400 MHz or a Mercury 300 MHz NMR spectrometer. Elemental analyses (CHN) were obtained from an Elementar vario EL III analyzer. Mass spectrometry was performed on a Finnigan/Thermo Quest MAT 95XL instrument using electron impact ionization for organic compounds and fast atom bombardment for metal complexes.

3.2. Synthetic Procedures

3.2.1. Synthesis of 4-Chlorophenylbenzoxazole, (4-cpboH)

The benzoxazole derivative ligand 4-cpboH was prepared using Philips' condensation as follows: 1 equivalent of 4-chlorobenzoic acid and 1.05 equivalent of 2-aminophenol were added to polyphosphoric acid (10 g/mmol of 4-chlorobenzoic acid), and then the mixture was stirred at 200 °C for 5 h. After cooling to room temperature, the mixture was slowly poured into pure water and stirred thoroughly; the precipitate was collected by filtration, washed with pure water (3×100 mL), and dried to obtain a crude product. The crude product was purified by silica gel column chromatography with n-hexane-dichloromethane (1:1~1:5) as the eluent to obtain the pure product.

Yield: 85%. ^1H NMR (300 MHz, CDCl_3 , 298 K; δ (ppm)): 7.74–7.80 (m, 3H), 7.56–7.59 (m, 1H), 7.36–7.41 (m, 2H), 6.96–7.00 (m, 1H). ^{13}C NMR (75 MHz, CDCl_3 , 298 K; δ (ppm)): 161.4, 151.3, 138.4, 137.2, 129.2, 128.2, 128.1, 127.6, 124.3, 119.9, 110.6. Anal. Calcd for $\text{C}_{13}\text{H}_8\text{ClNO}$ (MW = 229.66): C, 67.98; H, 3.51; N, 6.10. Found: C, 67.50; H, 3.48; N, 5.99%. MS (m/z): 229.6605.

3.2.2. Synthesis of $[(4\text{-cpbo})_2\text{Ir}(\mu\text{-Cl})]_2$

The cyclometalated Ir(III) chloride-bridged dimer $[(4\text{-cpbo})_2\text{Ir}(\mu\text{-Cl})]_2$ was synthesized according to a previous paper. A mixture of 2-ethoxyethanol and water (3:1, v/v) was added to a flask containing iridium trichloride ($\text{IrCl}_3 \cdot 3\text{H}_2\text{O}$, 2 mmol) and 4-cpboH (5 mmol), and the mixture was refluxed for 24 h under nitrogen. After cooling to room temperature, the mixture was poured into 20 mL of pure water, and the dimer precipitate was filtered off, washed with deionized water, and followed by drying at 60 °C in a vacuum oven.

Yield: 75%. ^1H NMR (300 MHz, DMSO-d_6 , 298 K; δ (ppm)): 7.71 (d, $J = 8.5$, 2H), 7.59 ((dd, $J = 8.5$, 4.3 Hz, 1H), 7.53 (d, $J = 8.5$ Hz, 1H), 7.50 (dd, $J = 8.5$, 4.3 Hz, 1H), 7.28 (dt, $J = 5.6$, 4.3 Hz, 1H), 7.22 (dt, $J = 5.6$, 4.3 Hz, 1H). ^{13}C NMR (75 MHz, CDCl_3 , 298 K; δ (ppm)): 163.7, 155.3, 139.1, 167.5, 134.6, 134.4, 131.6, 130.6, 130.1, 123.3, 123.2, 121.9, 112.6. Anal. Calcd for $\text{C}_{52}\text{H}_{28}\text{Cl}_6\text{Ir}_2\text{N}_4\text{O}_4$: C, 45.58; H, 2.06; N, 4.09. Found: C, 45.89; H, 2.08; N, 3.98%. MS (FAB; m/z): 1372.0320

3.2.3. Synthesis of Compound 1, $[(4\text{-cpbo})\text{Ir}(\mu\text{-Cl})(\mu\text{-O})\text{Ir}(4\text{-cpbo})]$

A flask was charged with 100 mg of $[(4\text{-cbo})_2\text{Ir}(\mu\text{-Cl})]_2$, 50 mg of anhydrous potassium carbonate, and 20 mL of acetone. The solution was stirred and warmed to 60 °C for 72 h. The precipitate dimer was filtered off and recrystallized from acetone.

Experimental data for 1: Yield: 60% based on iridium. Anal. Calcd for $\text{C}_{52}\text{H}_{28}\text{Cl}_5\text{Ir}_2\text{N}_4\text{O}_5 \cdot 2((\text{CH}_3)_2\text{CO})$: C, 47.49; H, 2.74; N, 3.82. Found: C, 47.25; H, 2.70; N, 3.98%. MS (FAB; m/z): 1352.0610.

3.2.4. General Procedure for N-alkylation Reaction

Add 1 mmol of amine, 2 mmol of alcohol, and 0.018 mmol of complex 1 to a Schlenk tube and react at 120 °C for 48 h under nitrogen. Then, the reaction mixture was cooled down and the residue was purified by column chromatography using n-hexane/dichloromethane as eluent to allow for a pure product. The desired product has been fully characterized by ^1H , ^{13}C NMR, and MS spectroscopy.

Spectral Data of of N-benzylaniline (P₁): ¹H NMR (d-chloroform, 600 MHz) = 7.38–7.33 (m, Ar, 4H), 7.28–7.25 (m, Ar, 1H), 7.19–7.16 (m, Ar, 2H), 6.73–6.68 (t, Ar, 1H), 6.65–6.63 (d, Ar, 2H, JHH = 7.8 Hz), 4.33 (s, CH₂, 2H), 4.02 (br. S, NH, 1H). ¹³C NMR (d-Chloroform, 150 MHz) = 148.2, 139.4, 129.3, 128.7, 127.5, 127.3, 117.6, 112.8, 48.3. MS (ESI/CI): *m/z* = 183.02, Calculated for C₁₃H₁₃N: 183.26 g/mol. IR (FT ATR): ν = 3411 (w), 3023 (w), 1605 (m), 1508 (m), 1321 (w), 1262 (m), 732 (s) cm⁻¹

Spectral Data of of N-(*p*-chlorobenzyl)aniline (P₂): ¹H NMR (d-chloroform, 600 MHz) = 7.29 (s, 3H, Ar), 7.17–7.11 (m, 2H, Ar), 6.73–6.68 (m, 1H, Ar), 6.58–6.59 (m, 2H, Ar), 4.28 (d, 2H, JHH = 5.4 Hz), 4.05 (br. S, NH, 1H). ¹³C NMR (d-Chloroform, 150 MHz) = 147.8, 137.8, 132.9, 129.3, 128.8, 128.7, 117.8, 112.9, 47.506. MS (ESI/CI): *m/z* = 216.98, Calculated for C₁₃H₁₂NCl⁺ [M]⁺: 217.68 g/mol. IR (FT ATR): ν = 3418 (w), 3045 (w), 28,434 (w), 16,045 (s), 1498 (s), 1321 (m), 1254 (m), 1090 (m), 814 (m), 745 (s) cm⁻¹.

Spectral Data of of N-(4-methoxybenzyl)aniline (P₃): ¹H NMR (d-chloroform, 600 MHz) = 7.29–7.27 (d, JHH = 8.4 Hz, 2H, Ar), 7.18–7.15 (m, 2H, Ar), 6.88–6.86 (m, 2H, Ar), 6.72–6.69 (t, 1H, Ar), 6.63–6.62 (m, 2H, Ar), 4.24 (br. S, NH, 1H), 3.91 (d, JHH = 13.2 Hz, 1H), 3.79 (s, 3H). ¹³C NMR (d-Chloroform, 150 MHz) = 158.9, 148.2, 131.4, 129.3, 128.8, 117.5, 113.8, 112.8, 55.3, 47.8. MS (ESI/CI): *m/z* = 213.21, Calculated for C₁₄H₁₅NO⁺ [M]⁺: 213.28 g/mol. IR (FT ATR): ν = 3411 (w), 3028 (w), 2836 (w), 16,045 (s), 1508 (s), 1239 (s), 1172 (m), 1030 (m), 821 (m), 747 (s) cm⁻¹.

Spectral Data of of benzyl(4-methoxyphenyl)amine (P₄): ¹H NMR (d-chloroform, 600 MHz) = 7.37–7.32 (m, Ar, 4H), 7.27–7.25 (t, Ar, 1H), 6.77–6.76 (m, Ar, 2H), 6.59–6.60 (m, Ar, 2H), 4.27 (s, CH₂, 2H), 3.73 (s, CH₃, 3H). ¹³C NMR (CDCl₃, 150 MHz) δ (ppm) = 152.2, 142.5, 139.7, 128.6, 127.6, 127.2, 114.9, 114.1, 55.8, 49.3. MS (ESI/CI): *m/z* = 213.05, Calculated for C₁₄H₁₅NO⁺ [M]⁺: 213.28 g/mol. IR (FT ATR): ν = 3403 (w), 3030 (w), 2836 (w), 1515 (s), 1232 (s), 1179 (w), 1030 (m), 821 (m), 739 (m) cm⁻¹.

Spectral Data of of N-(4-chlorophenyl)benzylamine (P₅): ¹H NMR (d-chloroform, 600 MHz) = 7.34–7.20 (m, Ar, 4H), 7.11–7.07 (m, Ar, 2H), 6.55–6.5102 (m, Ar, 2H), 4.62 (s, 1H), 4.30, 4.29 (d, CH₂, 2H, JHH = 6.0 Hz), 4.05 (br. S, NH, 1H). ¹³C NMR (d-Chloroform, 150 MHz) = 146.7, 138.8, 128.9, 128.7, 127.5, 127.4, 127.1, 126.6, 122.1, 113.9, 54.5, 48.4. MS (ESI/CI): *m/z* = 217.14, Calculated for C₁₃H₁₂NCl⁺ [M]⁺: 217.70 g/mol. IR (FT ATR): ν = 3411 (w), 3030 (w), 2851 (w), 1597(s), 1498 (s), 1314 (m) 1179 (w), 1090 (w), 8134 (m), 7312 (m) cm⁻¹.

Spectral Data of of N-benzyl-(2-fluorophenyl)amine (P₆): ¹H NMR (d-chloroform, 600 MHz) = 7.38–7.33 (m, Ar, 4H), 7.29–7.240 (m, Ar, 1H), 6.99–6.93 (m, Ar, 2H), 6.6718–6.65 (m, Ar, 1H), 6.64–6.59 (m, Ar, 1H), 4.37–4.36 (d, 2H, JHH = 5.4 Hz), 4.31 (br. S, NH, 1H). ¹³C NMR (d-Chloroform, 150 MHz) = 152.3, 150.7, 138.9, 136.6, 128.7, 127.4, 124.6, 116.8, 114.5, 114.3, 112.3, 47.8. MS (ESI/CI): *m/z* = 202.08, Calculated for C₁₃H₁₂NF⁺ [M]⁺: 201.25 g/mol. IR (FT ATR): ν = 3433 (w), 3030 (w), 2926 (w), 1620 (m), 15,145 (s), 13,356 (m), 1247 (m), 1187 (m), 747 (s) cm⁻¹.

Spectral Data of of N-ethyl-N-phenylamine (P₇): ¹H NMR (d-chloroform, 600 MHz) = 7.25–7.15 (m, Ar, 2H), 6.69–6.67 (t, Ar, 1H), 6.59–6.59 (d, Ar, 2H, JHH = 7.8 Hz), 3.521 (br. S, NH, 1H), 3.10–3.09 (q, 2H), 0.93–0.82 (t, 3H). ¹³C NMR (d-Chloroform, 150 MHz) = 148.11, 129.9, 116.6, 112.2, 45.1, 15.7. MS (ESI/CI): *m/z* = 121.08, Calculated for C₈H₁₁N⁺ [M]⁺: 121.19 g/mol. IR (FT ATR): ν = 3411 (w), 3050 (w), 2925 (m), 2858 (m), 1605 (s), 1508 (s), 1463 (s), 1321 (m), 12,612 (m), 1148 (m), 1028 (s), 747 (s) cm⁻¹.

Spectral Data of of N-propylaniline (P₈): ¹H NMR (d-chloroform, 600 MHz) = 7.171–7.15 (m, Ar, 2H), 6.69–6.66 (t, Ar, 1H), 6.61–6.59 (t, Ar, 2H), 3.62 (br. S, NH, 1H), 3.08–3.06 (t, 2H), 1.65–1.61 (m, CH₂, 2H), 0.99–0.98 (t, 3H). ¹³C NMR (d-Chloroform, 150 MHz) = 148.5, 129.3, 117.1, 112.7, 45.8, 22.8, 11.7. MS (ESI/CI): *m/z* = 135.13, Calculated for C₉H₁₃N⁺ [M]⁺: 135.21 g/mol. IR (FT ATR): ν = 3411 (w), 3022.3 (w), 2963 (w), 2933 (w), 1605 (m), 1508 (m), 1321 (m), 1254 (m), 1148 (w), 866 (w), 747 (m) cm⁻¹.

Spectral Data of of N-(*n*-butyl)aniline (P₉): ¹H NMR (d-chloroform, 600 MHz) = 7.17–7.14 (m, Ar, 2H), 6.62–6.66 (m, Ar, 1H), 6.59–6.58 (m, Ar, 2H), 3.57 (br. S, NH, 1H), 3.11–3.080(t, 2H), 1.62–1.55 (m, 2H), 1.45–1.39 (m, 2H), 0.96–0.93 (t, 3H). ¹³C NMR

(d-Chloroform, 150 MHz) = 148.6, 129.2, 117.1, 112.7, 43.7, 31.7, 20.3, 13.4. MS (ESI/CI): m/z = 149.09, Calculated for $C_{10}H_{15}N^+$ [M]⁺: 149.24 g/mol. IR (FT ATR): ν = 3418 (w), 3052 (w), 2933 (m), 2866 (m), 1605 (s), 1508 (s), 1321 (m), 1262 (m), 739 (s) cm^{-1} .

Spectral Data of of N-hexylaniline (P₁₀): ¹H NMR (d-chloroform, 600 MHz) = 7.17–7.14 (m, Ar, 2H), 6.68–6.66 (m, Ar, 1H), 6.59–6.58 (m, Ar, 2H), 3.57 (br. S, NH, 1H), 3.11–3.0718 (t, 2H), 1.62–1.55 (m, 2H), 1.45–1.39 (m, 2H), 0.96–0.93 (t, 3H). ¹³C NMR (d-Chloroform, 150 MHz) = 148.6, 129.2, 117.7, 112.7, 43.7, 31.7, 28.8, 27.4, 23.3, 134.0. MS (ESI/CI): m/z = 177.17, Calculated for $C_{12}H_{19}N^+$ [M]⁺: 177.29 g/mol. IR (FT ATR): ν = 3401 (w), 3058 (w), 2926 (m), 2856 (w), 1605 (s), 1508 (s), 1321(m), 1254 (m), 1179 (w), 8656 (w), 7470(s) cm^{-1} .

Spectral Data of of N-Isopropylaniline (P₁₁): ¹H NMR (d-chloroform, 600 MHz) = 7.16–7.14 (m, Ar, 2H), 6.70–6.68 (m, Ar, 1H), 6.61–6.59 (m, Ar, 2H), 3.40–3.37 (m, 1H), 1.10–1.09 (d, 6H). ¹³C NMR (d-Chloroform, 150 MHz) = 148.5, 129.3, 117.1, 112.7, 51.9, 21.9. MS (ESI/CI): m/z = 135.23, Calculated for $C_9H_{13}N^+$ [M]⁺: 135.21 g/mol. IR (FT ATR): ν = 3396 (w), 3058 (w), 1635 (m), 1582 (s), 1463 (m), 1269 (m), 739 (s) cm^{-1} .

Spectral Data of of N-Isopropyl-p-anisidine (P₁₂): ¹H NMR (d-chloroform, 600 MHz) = 7.51–7.49 (m, Ar, 2H), 6.97–6.94 (m, Ar, 2H), 4.50–4.44 (m, 1H), 1.10–1.09 (d, 6H). ¹³C NMR (CDCl₃, 150 MHz) δ (ppm) = 154.2, 147.5, 142.6, 130.7, 55.9, 52.9, 49.6, 22.1. MS (ESI/CI): m/z = 165.23, Calculated for $10H_{15}ON^+$ [M]⁺: 165.24 g/mol. IR (FT ATR): ν = 3366 (w), 2963 (w), 1618 (w), 1508 (s), 1232 (s), 1172 (m), 10,378 (m), 821 (m) cm^{-1} .

Spectral Data of of 4-Methoxy-N-(1-phenylethyl)aniline (P₁₃): ¹H NMR (d-chloroform, 600 MHz) = 7.51–7.49 (m, Ar, 2H), 7.19–7.17 (m, Ar, 2H), 6.90–6.66 (m, Ar, 3H), 6.62–6.59 (m, Ar, 2H), 4.21–4.18 (q, 1H). ¹³C NMR (d-Chloroform, 150 MHz) = 154.2, 148.6, 147.5, 142.6, 130.7, 129.2, 117.2, 112.617, 50.4, 30.9. MS (ESI/CI): m/z = 227.17, Calculated for $C_{15}H_{17}NO^+$ [M]⁺: 227.31 g/mol. IR (FT ATR): ν = 3388 (m), 3217 (w), 2918 (m), 2844 (w), 1635 (m), 1508 (s), 1463 (s), 1299 (w), 1232 (s), 1127 (w), 1028 (s), 821 (s) cm^{-1} .

Spectral Data of of N-methyl-N-phenyl-benzenemethanamine (P₁₄): ¹H NMR (d-chloroform, 600 MHz) = 7.36–7.31 (m, Ar, 4H), 7.26–7.23 (m, Ar, 1H), 7.16–7.14 (m, Ar, 2H), 6.71–6.68 (t, Ar, 1H), 6.67–6.64 (d, Ar, 2H, JHH = 7.8Hz), 4.36 (s, CH₂, 2H), 3.11 (s, 3H). ¹³C NMR (d-Chloroform, 150 MHz) = 148.8, 139.9, 129.7, 128.9, 127.9, 127.6, 117.3, 112.6, 48.1, 45.8. MS (ESI/CI): m/z = 197.07, Calculated for $C_{14}H_{15}N^+$ [M]⁺: 197.22 g/mol. IR (FT ATR): ν = 30,298 (w), 2925 (w), 2858 (w), 1597 (s), 1498 (s), 1456 (m), 13510 (m), 1112 (m), 1028 (m), 9401 (m), 747 (s), 724 (s) cm^{-1} .

Spectral Data of of N,N-dibenzylaniline (P₁₅): ¹H NMR (d-chloroform, 600 MHz) = 7.32–7.30 (m, Ar, 4H), 7.25–7.23 (m, Ar, 6H), 7.17–7.14 (m, Ar, 2H), 6.73–6.66 (m, Ar, 2H), 4.64–4.61 (d, Ar, 2H, JHH = 23.4 Hz). ¹³C NMR (d-Chloroform, 150 MHz) = 149.2, 138.6, 129.2, 128.7, 126.9, 126.7, 116.7, 112.4, 54.2. MS (ESI/CI): m/z = 273.21, Calculated for $C_{20}H_{19}N^+$ [M]⁺: 273.38 g/mol. IR (FT ATR): ν = 3038 (w), 2918 (m), 1597 (s), 1499 8 (s), 1456 (m), 1359 (m) 12,312 (m), 1028 (w), 956 (m), 732 (s) cm^{-1} .

Spectral Data of of N-phenylpyrrolidine (P₁₆): ¹H NMR (d-chloroform, 600 MHz) = 7.26 (m, 2H), 7.12 (m, 1H), 6.84 (m, 1H), 3.19–3.18 (m, 4H), 2.33 (s, 3H), 1.94–1.92 (m,4H). ¹³C NMR (d-Chloroform, 150 MHz) = 148.6, 129.7, 115.8, 111.97, 47.9, 26.0. MS (ESI/CI): m/z = 147.13, Calculated for $C_{13}H_{13}N$: 147.23 g/mol. IR (FT ATR): ν = 3058 (w), 3028 (w), 2963 (m), 2926 (s), 2836 (m), 1605 (m), 15,967 (s), 1508 (s), 1463 (m), 1366 (s), 1357 (w), 1239 (w), 11,867 (m), 1157 (m), 993 (m), 7467 (s), 6869 (s) cm^{-1} .

Spectral Data of of N-(4-chlorophenyl) pyrrolidine (P₁₇): ¹H NMR (d-chloroform, 600 MHz) = 7.26–7.64 (m, 2H), 6.58–6.95 (m, 2H), 3.86–3.76 (m, 4H), 2.54–2.51 (m, 4H). ¹³C NMR (d-Chloroform, 150 MHz) = 147.5, 130.01, 121.3, 113.6, 48.7, 26.3. MS (ESI/CI): m/z = 181.22, Calculated for $C_{11}H_{12}NCl^+$ [M]⁺: 181.67 g/mol. FTIR (ATR): ν = 2963 (w), 2926 (s), 2858 (m), 1739 (s), 1605 (m), 1471 (m), 1463 (m), 1374 (s), 276 (w), 1232 (s), 1157 (w), 1075 (w), 1015 (w), 799 (m) cm^{-1} .

Spectral Data of of N-(4-methoxyphenyl) pyrrolidine (P₁₈): ¹H NMR (d-chloroform, 600 MHz) = 6.87 (d, J = 9.0 Hz, 2H), 6.55 (d, J = 9.0 Hz, 2H), 3.767 (s, 3H), 3.23 (t, J = 6.5 Hz, 4H), 2.02–1.99 (m, 4H). ¹³C NMR (d-Chloroform, 150 MHz) = 116.3, 113.2, 57.1, 49.3, 26.21. MS (ESI/CI): m/z = 177.256, Calculated for $C_{11}H_{15}NO^+$ [M]⁺: 177.25 g/mol. FTIR (ATR):

$\nu = 3045$ (w), 2948 (m), 2926(s), 2856(m), 1620 (w), 1515 (m), 1485 (w), 1463 (m), 1366 (m), 1276 (w), 1239 (m), 1179 (w), 1157 (w), 1045 (m), 971 (w), 806 (s), 732 (w) cm^{-1} .

Spectral Data of of N-phenylpiperidine (P₁₉): ^1H NMR (d-chloroform, 600 MHz) = 7.45 (t, 2H, J = 7.4 Hz), 6.99 (d, 2H, J = 7.8 Hz), 6.73 (t, 1H, J = 7.3 Hz), 3.36 (t, 4H, J = 6.7 Hz), 1.81 (m, 4H), 1.62 (t, 2H, J = 4.8 Hz). ^{13}C NMR (CDCl_3 , 150 MHz) δ (ppm) = 152.6, 129.9, 119.7, 117.3, 60.12, 26.6, 24.9. MS (ESI/CI): $m/z = 161.12$, Calculated for $\text{C}_{11}\text{H}_{15}\text{N}^+$ [M] $^+$: 161.25 g/mol. IR (FT ATR): $\nu = 2933$ (m), 2854 (m), 2806 (m), 1598 (s), 1495 (s), 1451 (m), 1385 (m), 1236 (s), 1221 (s), 1132 (m), 918 (m), 754 (s) cm^{-1} .

Spectral Data of of 1-(piperidine-1-yl) pyridine (P₂₀): ^1H NMR (d-chloroform, 600 MHz) = 8.28 (ddd, 1H), 7.62 (ddd, 1H), 6.85 (dd, 1H), 6.76 (ddd, 4H), 1.86 (td, 6H). ^{13}C NMR (d-Chloroform, 150 MHz) = 156.0, 148.2, 137.5, 112.6, 107.3, 46.6, 25.8, 25.0. MS (ESI/CI): $m/z = 162.21$, Calculated for $\text{C}_{10}\text{H}_{14}\text{N}_2^+$ [M] $^+$: 162.24 g/mol. FTIR (ATR): $\nu = 3008$ (w), 2926 (m), 2851 (m), 1597 (s), 1485 (s), 1433 (s), 1381 (w), 1314 (m), 1247 (s), 1157 (w), 1127 (m), 1023 (w), 8501 (w), 769 (s), 733 (w) cm^{-1} .

Spectral Data of of 1-methyl-4-(pyridin-2-yl) piperazine (P₂₁): ^1H NMR (d-chloroform, 600 MHz) = 8.21 (dd, 1H), 7.66 (ddd, 1H), 6.88–6.78 (m, 2H), 3.74–3.66 (m, 4H), 3.22–3.13 (m, 4H). ^{13}C NMR (d-Chloroform, 150 MHz) = 160.4, 147.9, 137.6, 110.1, 107.2, 46.1, 45.8. MS (ESI/CI): $m/z = 177.23$, Calculated for $\text{C}_{10}\text{H}_{15}\text{N}_3^+$ [M] $^+$: 177.245 g/mol. IR (ATR): $\nu = 3329$ (s), 2933 (m), 2866 (m), 1627 (m), 1605 (s), 1530 (w), 1515 (s), 1448 (m), 1157 (w), 1053 (m), 1030 (w), 888 (w), 859 (w), 769 (s), 702 (w) cm^{-1} .

3.2.5. Intermolecular Cyclization to Synthesize Cyclizine

In a Schlenk tube, 1 mmol of N-methyldiethanolamine (MDEA) was mixed with 2 mmol of diphenylmethanamine and complex **1**, and the reaction was carried at 140 °C for 48 h under nitrogen. The product cyclizine was purified by column chromatography with an isolated yield of 60%. It was fully characterized by ^1H , ^{13}C NMR, and MS spectroscopy.

^1H NMR (d-chloroform, 600 MHz) = 7.45–7.18 (m, 10H, Ph), 4.27 (s, 1H, N-CH), 3.32 (s, 8H, N-CH), 2.31 (s, 3H, N-CH₃). ^{13}C NMR (d-Chloroform, 150 MHz) = 144.0, 129.7, 129.0, 128.5, 77.5, 56.1, 52.4, 45.7. MS (ESI/CI): $m/z = 266.12$, Calculated for $\text{C}_{18}\text{H}_{22}\text{N}_2$ [M] $^+$: 266.38 g/mol. FTIR (ATR): $\nu = 3060$ (w), 3030 (w), 2926 (m), 2858 (w), 1620 (s), 1493 (m), 1448 (m), 1276 (m), 1150 (w), 1075 (w), 1030 (w), 985 (w), 926 (w), 859 (w), 747 (s), 702 (s) cm^{-1} .

3.3. Electron Paramagnetic Resonance (EPR)

EPR was measured with a Bruker EMX-10/12 spectrometer. The samples were dissolved in toluene. EPR settings: field, center field 3520.000 G, sweep width 100.000 G, resolution 2048 points; microwave frequency, 9.879 GHz; microwave power, 10.080 mW; number of scans, 1.

3.4. Single-Crystal X-ray Diffraction

All the crystals were obtained from a mixed solution of dichloromethane and n-hexane. The diffraction data for complex **1** was collected on a Bruker SMART APEX CCD diffractometer with a graphite-monochromatized MoK α X-ray radiation ($\lambda = 0.71073$ Å) at 110 K. All the calculations for the structural determination were carried out using a SHELXS-97 package. The positions of the heavy atoms, including the iridium atoms, were located using the direct method. The remaining atoms were found in a series of alternating difference Fourier maps and least-square refinement. The crystallographic data for all the structures reported here have been deposited in the Cambridge Data Centre as supplementary publication number CCDC 2100518.

Supplementary Materials: The following supporting information can be downloaded at: <https://www.mdpi.com/article/10.3390/inorganics10120237/s1>. Table S1: The Atomic Coordinates (angstroms) of Complex **1**.

Author Contributions: Conceptualization, T.-R.C.; Methodology, Y.-S.C., Y.-H.L., Y.-T.C. and T.-R.C.; Y.-S.C., Y.-H.L. and Y.-T.C.; Investigation, Y.-S.C., Y.-H.L., Y.-T.C. and T.-R.C.; Resources, C.-Y.L.; Data Curation, Y.-S.C., Y.-H.L., Y.-T.C. and T.-R.C.; Writing—Review and Editing, T.-R.C. and C.-Y.L.; Project Administration, T.-R.C. All authors have read and agreed to the published version of the manuscript.

Funding: This research received no external funding.

Data Availability Statement: Not applicable.

Acknowledgments: This work was supported by the Ministry of Science and Technology (MOST 109-2622-M-153-001-CC3). The authors would like to thank the Instrument Center of National Chung Hsing University for the single-crystal X-ray structure determination and help with measurements of Nuclear Magnetic Resonance and LC-MS/MS (MOST 108-2731-M-005-001).

Conflicts of Interest: The funders had no role in the design of the study; in the collection, analyses, or interpretation of data; in the writing of the manuscript; or in the decision to publish the results.

References

1. Roy, S.; Das, S.K.; Khatua, H.; Das, S.; Chattopadhyay, B. Road Map for the Construction of High-Valued N-Heterocycles via Denitrogenative Annulation. *Acc. Chem. Res.* **2021**, *54*, 4395–4409. [[CrossRef](#)] [[PubMed](#)]
2. Mondal, S.; Dumur, F.; Gimes, D.; Sibi, M.P.; Bertr, M.P.; Nechab, M. Enantioselective Radical Reactions Using Chiral Catalysts. *Chem. Rev.* **2022**, *122*, 5842–5967. [[CrossRef](#)] [[PubMed](#)]
3. Wang, Y.; Wen, X.; Cui, X.; Wojtas, L.; Zhang, X.P. Asymmetric Radical Cyclopropanation of Alkenes with In Situ-Generated Donor-Substituted Diazo Reagents via Co(II)-Based Metalloradical Catalysis. *J. Am. Chem. Soc.* **2017**, *139*, 1049–1052. [[CrossRef](#)] [[PubMed](#)]
4. Zhang, C.; Wang, D.-S.; Lee, W.-C.C.; McKillop, A.M.; Zhang, X.P. Controlling Enantioselectivity and Diastereoselectivity in Radical Cascade Cyclization for Construction of Bicyclic Structures. *J. Am. Chem. Soc.* **2021**, *143*, 11130–11140. [[CrossRef](#)] [[PubMed](#)]
5. Xie, J.; Xu, P.; Zhu, Y.; Wang, J.; Lee, W.-C.C.; Zhang, X.P. New Catalytic Radical Process Involving 1,4-Hydrogen Atom Abstraction: Asymmetric Construction of Cyclobutanones. *J. Am. Chem. Soc.* **2021**, *143*, 11670–11678. [[CrossRef](#)]
6. Zhou, M.; Wolzak, L.A.; Li, Z.; de Zwart, F.J.; Mathew, S.; de Bruin, B.J. Catalytic Synthesis of 1H-2-Benzoxocins: Cobalt(III)-Carbene Radical Approach to 8-Membered Heterocyclic Enol Ethers. *Am. Chem. Soc.* **2021**, *143*, 20501–20512. [[CrossRef](#)]
7. Ke, J.; Lee, W.-C.C.; Wang, X.; Wang, Y.; Wen, X.; Zhang, X.P.J. Metalloradical Activation of In Situ-Generated α -Alkynyldiazomethanes for Asymmetric Radical Cyclopropanation of Alkenes. *Am. Chem. Soc.* **2022**, *144*, 2368–2378. [[CrossRef](#)]
8. Yu, M.; Fu, X.J. Visible Light Promoted Hydroxylation of a Si–C(sp³) Bond Catalyzed by Rhodium Porphyrins in Water. *Am. Chem. Soc.* **2011**, *133*, 15926–15929. [[CrossRef](#)]
9. Li, G.; Han, A.; Pulling, M.E.; Estes, D.P.; Norton, J.R. Evidence for Formation of a Co–H Bond from (H₂O)₂Co(dmgbF₂)₂ under H₂: Application to Radical Cyclizations. *J. Am. Chem. Soc.* **2012**, *134*, 14662–14665. [[CrossRef](#)]
10. Zhang, Q.; Wang, S.; Zhang, Q.; Xiong, T.; Zhang, Q. Radical Addition-Triggered Remote Migratory Isomerization of Unactivated Alkenes to Difluoromethylene-Containing Alkenes Enabled by Bimetallic Catalysis. *ACS Catal.* **2022**, *12*, 527–535. [[CrossRef](#)]
11. Stevens, H.; Duan, P.-C.; Dechert, S.; Meyer, F. Competing H₂ versus Intramolecular C–H Activation at a Dinuclear Nickel Complex via Metal–Metal Cooperative Oxidative Addition. *J. Am. Chem. Soc.* **2020**, *142*, 6717–6728. [[CrossRef](#)]
12. Ott, J.C.; Bürgy, D.; Guan, H.; Gade, L.H. 3d Metal Complexes in T-shaped Geometry as a Gateway to Metalloradical Reactivity. *Acc. Chem. Res.* **2022**, *55*, 857–868. [[CrossRef](#)]
13. Chen, J.; Liang, Y.-J.; Wang, P.-Z.; Li, G.-Q.; Zhang, B.; Qian, H.; Huan, X.-D.; Guan, W.; Xiao, W.-J.; Chen, J.-R. Photoinduced Copper-Catalyzed Asymmetric C–O Cross-Coupling. *J. Am. Chem. Soc.* **2021**, *143*, 13382–13392. [[CrossRef](#)]
14. Lee, H.; Ahn, J.M.; Oyala, P.H.; Citek, C.; Yin, H.; Fu, G.C.; Peters, J.C. Investigation of the C–N Bond-Forming Step in a Photoinduced, Copper-Catalyzed Enantioconvergent N–Alkylation: Characterization and Application of a Stabilized Organic Radical as a Mechanistic Probe. *J. Am. Chem. Soc.* **2022**, *144*, 4114–4213. [[CrossRef](#)]
15. Sinha, S.K.; Guin, S.; Maiti, S.; Biswas, J.P.; Porey, S.; Maiti, D. Toolbox for Distal C–H Bond Functionalizations in Organic Molecules. *Chem. Rev.* **2022**, *122*, 5682–5841. [[CrossRef](#)]
16. Wang, X.; Ke, J.; Zhu, Y.; Deb, A.; Xu, Y.; Zhang, X.P. Asymmetric Radical Process for General Synthesis of Chiral Heteroaryl Cyclopropanes. *J. Am. Chem. Soc.* **2021**, *143*, 11121–11129. [[CrossRef](#)]
17. Hu, Y.; Lang, K.; Li, C.; Gill, J.B.; Kim, I.; Lu, H.; Fields, K.B.; Marshall, M.; Cheng, Q.; Cui, X.; et al. Enantioselective Radical Construction of 5-Membered Cyclic Sulfonamides by Metalloradical C–H Amination. *J. Am. Chem. Soc.* **2019**, *141*, 18160–18169. [[CrossRef](#)]
18. Juliá, F.; Constantin, T.; Leonori, D. Applications of Halogen-Atom Transfer (XAT) for the Generation of Carbon Radicals in Synthetic Photochemistry and Photocatalysis. *Chem. Rev.* **2022**, *122*, 2292–2352. [[CrossRef](#)]
19. Jia, Z.; Zhang, L.; Luo, S. Asymmetric C–H Dehydrogenative Allylic Alkylation by Ternary Photoredox-Cobalt-Chiral Primary Amine Catalysis under Visible Light. *J. Am. Chem. Soc.* **2022**, *144*, 10705–10710. [[CrossRef](#)]

20. Hershberger, J.W.; Klingler, R.J.; Kochi, J.K. Electron-transfer catalysis. Radical chain mechanism for the ligand substitution of metal carbonyls. *J. Am. Chem. Soc.* **1982**, *104*, 3034–3043.
21. Chen, T.-R.; Lee, H.-P.; Chen, J.-D.; Chen, K.H.-C. An 18+ δ iridium dimer releasing metalloradicals spontaneously. *Dalton Trans.* **2010**, *39*, 9458–9461. [[CrossRef](#)] [[PubMed](#)]
22. Klein, A.; Vogler, C.; Kaim, W. Organometallics, The δ in 18 + δ Electron Complexes: Importance of the Metal/Ligand Interface for the Substitutional Reactivity of “Re(0)” Complexes (α -diimine-)ReI(CO)3(X). *Organometallics* **1996**, *15*, 236–244. [[CrossRef](#)]
23. Mao, F.; Schut, D.M.; Tyler, D.R. Catalysis by 18 + δ compounds. Cyclooligomerization of acetylenes catalyzed by Co(CO)3L2 Organometallics. *Organometallics* **1996**, *15*, 4770–4775. [[CrossRef](#)]
24. Powell, D.A.; Ramsden, P.D.; Batey, R.A. Phase-Transfer-Catalyzed Alkylation of Guanidines by Alkyl Halides under Biphasic Conditions: A Convenient Protocol for the Synthesis of Highly Functionalized Guanidines. *J. Org. Chem.* **2003**, *68*, 2300–2309. [[CrossRef](#)] [[PubMed](#)]
25. Yang, Y.-S.; Shen, Z.-L.; Loh, T.-P. Indium (Zinc)-Copper-Mediated Barbier-Type Alkylation Reaction of Nitrones in Water: Synthesis of Amines and Hydroxylamines. *Org. Lett.* **2009**, *11*, 1209–1212. [[CrossRef](#)]
26. Mirabdolbaghi, R.; Dudding, T. Expanding the Forefront of Strong Organic Brønsted Acids: Proton-Catalyzed Hydroamination of Unactivated Alkenes and Activation of Au(I) for Alkyne Hydroamination. *Org. Lett.* **2015**, *17*, 1930–1933. [[CrossRef](#)]
27. Blicek, R.; Bahri, J.; Taillefer, M.; Monnier, F. Copper-Catalyzed Hydroamination of Terminal Allenes. *Org. Lett.* **2016**, *18*, 1482–1485. [[CrossRef](#)]
28. Zhao, X.; She, Y.; Fang, K.; Li, G. CuCl-Catalyzed Ullmann-Type C–N Cross-Coupling Reaction of Carbazoles and 2-Bromopyridine Derivatives. *J. Org. Chem.* **2017**, *82*, 1024–1033. [[CrossRef](#)]
29. Yoo, W.-J.; Tsukamoto, T.; Kobayashi, S. Visible Light-Mediated Ullmann-Type C–N Coupling Reactions of Carbazole Derivatives and Aryl Iodides. *Org. Lett.* **2015**, *17*, 3640–3642. [[CrossRef](#)]
30. Lee, D.-H.; Taher, A.; Hossain, S.; Jin, M.-J. An Efficient and General Method for the Heck and Buchwald_Hartwig Coupling Reactions of Aryl Chlorides. *Org. Lett.* **2011**, *13*, 5540–5543. [[CrossRef](#)]
31. Mitsudo, K.; Shimohara, S.; Mizoguchi, J.; Mandai, H.; Suga, S. Synthesis of Nitrogen-Bridged Terthiophenes by Tandem Buchwald_Hartwig Coupling and Their Properties. *Org. Lett.* **2012**, *14*, 2702–2705. [[CrossRef](#)]
32. Chen, T.-R.; Chen, Y.-T.; Chen, Y.-S.; Lee, W.-J.; Lin, Y.-H.; Wang, H.-C. Iridium/graphene nanostructured catalyst for the N-alkylation of amines to synthesize nitrogen-containing derivatives and heterocyclic compounds in a green process. *RSC Adv.* **2022**, *12*, 4760–4770. [[CrossRef](#)]
33. Chen, T.-R. Synthesis and characterization of cyclometalated iridium(III) complexes containing benzoxazole derivatives and different ancillary ligands. *J. Organomet. Chem.* **2008**, *693*, 3117–3130. [[CrossRef](#)]
34. Thiagarajan, S.; Gunanathan, C. Direct Catalytic Symmetrical, Unsymmetrical N,N-Dialkylation and Cyclization of Acylhydrazides Using Alcohols. *Org. Lett.* **2020**, *22*, 6617–6622. [[CrossRef](#)]
35. Yuan, K.; Jiang, F.; Sahli, Z.; Achard, M.; Roisnel, T.; Bruneau, C. Iridium-Catalyzed Oxidant-Free Dehydrogenative C-H Bond Functionalization: Selective Preparation of N-Arylpiperidines through Tandem Hydrogen Transfers, *Angew. Chem. Int. Ed.* **2012**, *51*, 8876–8880. [[CrossRef](#)]
36. Zou, Q.; Wang, C.; Smith, J.; Xue, D.; Xiao, J. Alkylation of Amines with Alcohols and Amines by a Single Catalyst under Mild Conditions. *Chem.—Eur. J.* **2015**, *21*, 9656–9661. [[CrossRef](#)]
37. Blank, B.; Kempe, R.J. Catalytic Alkylation of Methyl-N-Heteroaromatics with Alcohols. *Am. Chem. Soc.* **2010**, *132*, 924–925. [[CrossRef](#)]
38. Eka Putra, A.; Oe, Y.; Ohta, T. Ruthenium-Catalyzed Enantioselective Synthesis of β -Amino Alcohols from 1,2-Diols by “Borrowing Hydrogen”. *Eur. J. Org. Chem.* **2013**, *2013*, 6146–6151. [[CrossRef](#)]
39. Balaraman, E.; Srimani, D.; Diskin-Posner, Y.; Milstein, D. Direct Synthesis of Secondary Amines From Alcohols and Ammonia Catalyzed by a Ruthenium Pincer Complex. *Catal. Lett.* **2015**, *145*, 139–144. [[CrossRef](#)]
40. Quintard, A.; Rodriguez, J. A Step into an eco-Compatible Future: Iron- and Cobalt-catalyzed Borrowing Hydrogen Transformation. *ChemSusChem* **2016**, *9*, 28–30. [[CrossRef](#)]
41. Santoro, F.; Psaro, R.; Ravasio, N.; Zaccheria, F. N-Alkylation of amines through hydrogen borrowing over a heterogeneous Cu catalyst. *RSC Adv.* **2014**, *4*, 2596–2600. [[CrossRef](#)]
42. Clubiey, M.; Henson, T.; Riddington, A.W.; Peck, C.B. Diazepam metabolism in human foetal and adult liver. *J. Clin. Pharmacol.* **1977**, *4*, 652–662.
43. Afanasyev, O.I.; Kuchuk, E.; Usanov, D.L. Chusov, Reductive Amination in the Synthesis of Pharmaceuticals. *D. Chem. Rev.* **2019**, *119*, 11857–11911. [[CrossRef](#)] [[PubMed](#)]
44. Abbenhuis, R.A.T.M.; Boersma, J.; van Koten, G. Ruthenium-Complex-Catalyzed N-(Cyclo)alkylation of Aromatic Amines with Diols. Selective Synthesis of N-(ω -Hydroxyalkyl)anilines of Type PhNH(CH₂)_nOH and of Some Bioactive Arylpiperazines. *J. Org. Chem.* **1998**, *63*, 4282–4290. [[CrossRef](#)]